

## Negative feedback self-regulation contributes to robust and high-fidelity transmembrane signal transduction

M Ángeles Serrano, Manuel Jurado and Ramon Reigada

*J. R. Soc. Interface* 2013 **10**, 20130581, published 21 August 2013

---

### References

**This article cites 19 articles, 5 of which can be accessed free**

<http://rsif.royalsocietypublishing.org/content/10/88/20130581.full.html#ref-list-1>

### Subject collections

Articles on similar topics can be found in the following collections

[biophysics](#) (261 articles)

[computational biology](#) (219 articles)

[systems biology](#) (132 articles)

### Email alerting service

Receive free email alerts when new articles cite this article - sign up in the box at the top right-hand corner of the article or click [here](#)



## Research

**Cite this article:** Serrano MÁ, Jurado M, Reigada R. 2013 Negative feedback self-regulation contributes to robust and high-fidelity transmembrane signal transduction. *J R Soc Interface* 10: 20130581. <http://dx.doi.org/10.1098/rsif.2013.0581>

Received: 1 July 2013

Accepted: 31 July 2013

### Subject Areas:

systems biology, biophysics, computational biology

### Keywords:

transmembrane signal transduction, signalling nanoclusters, high-fidelity transduction, mitogen-activated protein kinase pathway

### Author for correspondence:

Ramon Reigada

e-mail: [reigada@ub.edu](mailto:reigada@ub.edu)

# Negative feedback self-regulation contributes to robust and high-fidelity transmembrane signal transduction

M Ángeles Serrano<sup>1</sup>, Manuel Jurado<sup>2</sup> and Ramon Reigada<sup>2</sup>

<sup>1</sup>Departament de Física Fonamental, and <sup>2</sup>Departament de Química Física and Institut de Química Teòrica i Computacional (IQTCUB), Universitat de Barcelona, Martí i Franquès 1, 08028 Barcelona, Spain

We present a minimal motif model for transmembrane cell signalling. The model assumes signalling events taking place in spatially distributed nanoclusters regulated by a birth/death dynamics. The combination of these spatio-temporal aspects can be modulated to provide a robust and high-fidelity response behaviour without invoking sophisticated modelling of the signalling process as a sequence of cascade reactions and fine-tuned parameters. Our results show that the fact that the distributed signalling events take place in nanoclusters with a finite lifetime regulated by local production is sufficient to obtain a robust and high-fidelity response.

## 1. Introduction

Transmembrane cellular signalling pathways are responsible for linking external stimuli and internal cellular actions. Typically, signalling molecules activate specific receptor proteins on the cell membrane triggering a cascade of interactions that diffuse messengers inside the cell regulating its activity, growth and development. Signalling pathways not only sense information but also integrate and process it into fast (seconds to minutes) and robust high-fidelity responses [1]. The importance of certain ubiquitous motifs in signalling pathways—such as activation cascades and feedback loops—for this processing is well recognized. How spatio-temporal mechanisms influence signal transduction is much less understood.

The interplay between cascades and feedback loops can explain intriguing properties, for example opposing cell fate decisions, depending on different stimuli provoking different activation amplitudes [2–6]. As a striking example, the mitogen-activated protein kinase (MAPK) pathway governs crucial cellular processes like proliferation and differentiation [7], and its dysfunction has been related to cancer [8]. In short, the pathway consists of the sequential activation of three kinases. The transduction process is initiated by a growth factor-induced recruitment of the SOS factor to the plasma membrane that links and activates a G-protein. The latter recruits a MAPK kinase kinase (MAPKKK) from the cytosol to the plasma membrane, which double-phosphorylates and activates a MAPK kinase (MAPKK) that, in turn, double-phosphorylates and activates a MAPK as a final signalling messenger. The most known example of this MAPK cascade corresponds to the regulation of ERK (MAPK), which features Ras as the G-protein, Raf as the MAPKKK and MEK as the MAPKK [7]. Mathematical models have shown that, in the absence of feedback regulation, the MAPK cascade elicits a steep response to the input signal if successive protein activations are performed in a distributive manner [9], while feedback regulations modulate the overall sensitivity of the pathway [10,11].

Recently, membrane nanocluster-concentrating signalling proteins have been proposed as a new fundamental mechanism to modulate and increase the efficiency and specificity of the MAPK cascade [12,13]. The work by Harding & Hancock [14] has revealed that activated receptor proteins aggregate in the membrane forming nanoclusters that recruit the downstream factors (Raf, MEK and ERK) from the cytosol and perform signal transduction. These signalling

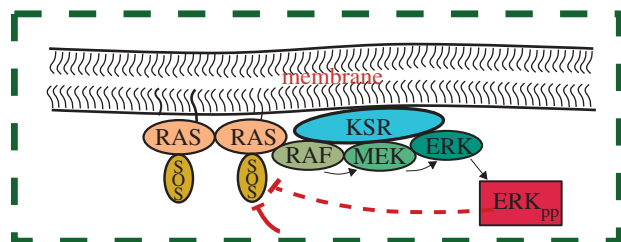


**Figure 1.** Sketch of the Ras–MAPK signalling platform as described in the literature [7,14]. Negative feedback regulations with two different origins have been represented with thick lines: the solid one corresponds to an external regulation, whereas the dashed one stands for an internal self-regulation. (Online version in colour.)

platforms (figure 1) display two important spatio-temporal characteristics: they are transient with short lifetimes (typically under 1 s) and dispersed in the cell membrane occupying a small reaction volume (radii  $\approx 10$  nm) [14]. When the nanocluster spatial organization is combined with the corresponding cascades and feedback loops, *in silico* and *in vivo* analyses of MAPK signalling show that the system is able to perform high-fidelity signal transduction. The numerical implementation of the latter proposal by Tian *et al.* [15] shows that in a range of kinetic parameters, nanoclusters work as switches responding maximally to very low-input signals. As the generation of signalling platforms is proportional to the input stimulus, nanocluster ultrasensitivity results in high-fidelity signal transduction (the global response is proportional to the stimulus). Despite the undeniable relevance of the work of Tian *et al.* [15], a critical analysis of the contribution of the spatio-temporal nanocluster dynamics on the signal/response behaviour is missing. The intricacy of the signalling cascade and high number of tuned-for-ultrasensitivity parameters in that *in silico* approach hinders to discriminate the role of the spatio-temporal nanocluster dynamics in signalling output.

In this paper, we consider a remarkably simple and generic motif model that incorporates the aggregation of signalling proteins into discrete transient domains but that simplifies the pathway structure to unveil the importance of the spatio-temporal dynamics of membrane nanoclusters. We want to emphasize that nanocluster dynamics may control the general stimulus/response behaviour of signalling processes involving dispersed signalling platforms, regardless of the particular architecture of their signalling circuits. Interestingly, we find that complex behaviours attributed to the particular architecture—cascades of distributed activations and feedback loops—of signalling pathways can also be achieved by regulating the spatio-temporal dynamics of nanoclusters encapsulating much simpler signalling motifs. More specifically, ultrasensitivity of signalling platforms leading to high-fidelity transmission is found to be affected by their lifetime. To explore how cells might have protected the fidelity of signal transduction, two scenarios have been compared: a situation where the nanocluster lifetime is externally regulated, and the case where it is not prefixed but linked to their local activity (figure 1). In the latter case, we report that self-regulation induces individual switch-like behaviour and high-fidelity global responses even when the kinetic parameters are changed by orders of magnitude. This finding indicates that local nanocluster

self-regulation might be a design principle to achieve robust and high-fidelity transmembrane signal transduction.

## 2. The model

The description of complex signalling circuits such as those for the MAPK pathway is often performed by the combination of transformation reactions modelled as simple enzymatic processes. Therefore, the simplest way to describe the complex features of nanoclusters signal transduction is to model each nanocluster as a minimal signalling motif based on the standard Michaelis–Menten formulation,

$$\text{NC} + \text{S} \xrightleftharpoons[k_{-1}]{k_1} \text{NC} - \text{S} \xrightarrow{k_2} \text{P} + \text{NC}, \quad (2.1)$$

where NC, S, NC – S and P stand for the enzyme, substrate, intermediate and product species, respectively, and  $k_1$ ,  $k_{-1}$  and  $k_2$  are reaction rate constants. The role of the enzyme is assigned here to the nanocluster platform NC, where the activity of the signalling motif takes place. Typically, nanocluster platforms are transient structures assembled by anchored proteins in the inner leaflet of plasma membrane. These can be proteins-like GTPase Ras that become activated by mediation of the cytoplasmatic protein SOS as a catalyst when the external stimulus (e.g., growth factor) binds to membrane receptors. In the context of MAPK signalling, the first reversible reaction in equation (2.1) corresponds to the recruiting of Raf protein to immobile Ras nanoclusters and its subsequent activation, which starts the MAPK cascade, whereas the second (catalytic) step comprehends successive phosphorylation and activation of MEK and ERK kinases.

In our model, signalling nanoclusters are assumed to follow a dynamics that controls their number and lifetime. We first consider a birth/death mechanism that does not depend on the spatial distribution or the functioning of nanoclusters but represents some extrinsic regulation (model A, figure 2a). Nanoclusters are dynamically formed in the cell membrane at rate  $k_0$ , whereas, independently, a fixed constant rate  $k_3$  determines the frequency of nanocluster disassembling. During their lifetime, signalling nanoclusters can generate product molecules according to the reaction motif in equation (2.1). The external stimulus is represented by parameter  $\alpha$ , which is set to unity at maximal stimulus. The role of  $\alpha$  is twofold. First, *in vivo* experiments reveal that nanocluster generation is proportional to input growth factor concentration [15], so we consider the frequency of nanocluster formation to be proportional to the stimulus  $k_0 = \alpha k_0^{(m)}$ , where  $k_0^{(m)}$  corresponds to nanocluster generation rate at maximal stimulus. Second, the kinetics of the production reaction is also considered proportional to the stimulus  $k_2 = \alpha k_2^{(m)}$ , with  $k_2^{(m)}$  being the catalytic rate at maximal stimulus. This dependence indicates the existence of a generic positive feedback regulation in the signalling process that may account for different experimental evidences. For instance, it could fit the observed positive feedback regulation from Ras to SOS [16] that is known to enhance the switch-like behaviour of nanocluster response. It could also account for the fact that kinases are phosphorylated in separate encounters instead of occurring sequentially in a single encounter. Such distributive mechanism could also justify the latter dependence of  $k_2$  (see also references [9,15]).

In the numerical simulations, we follow a stochastic approach similar to the Gillespie algorithm [17,18]. All events

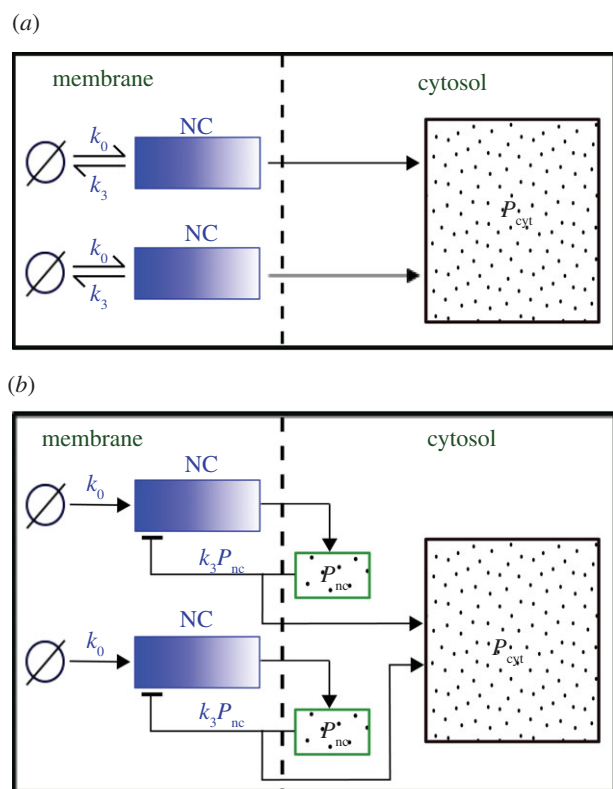


**Figure 2.** Schematic of the two proposed nanocluster (NC) disassembling mechanisms. (a) Model A: nanoclusters generate signalling output species that freely diffuse to the cytosol ( $P_{\text{cyt}}$ ). Their lifetime is regulated by a frequency determined externally ( $k_3$ ). (b) Model B: signalling output molecules transiently reside close to the nanocluster ( $P_{\text{nc}}$ ) and self-regulate its lifetime ( $k_3 P_{\text{nc}}$ ). In (a,b) only two nanoclusters are represented, but the number in our simulations is in order of hundreds. (Online version in colour.)

corresponding to nanocluster birth and death, and to internal molecular transformations, are treated as stochastic events because of the small numbers of proteins involved and the limited lifetime of signalling platforms. In particular, we consider Poissonian processes with a frequency determined by the corresponding rates, which can be found in literature. For the MAPK pathway, cytosolic concentration of Raf is about  $10^{-7}$  M [9], whereas Raf activation is of order  $\approx 10^6$ – $10^8$   $\text{M}^{-1} \text{s}^{-1}$  [3,11], which leads to a forward reaction rate  $k_1 \approx 0.1$ – $10$   $\text{s}^{-1}$ . The dissociation reaction is slower,  $k_{-1} \approx 10^{-2}$   $\text{s}^{-1}$  [3,11]. Catalytic constant rates corresponding to kinase phosphorylation processes are much larger,  $k_2 \approx 10$ – $100$   $\text{s}^{-1}$  [3,11,15]. Finally, the death rate  $k_3 = 2$   $\text{s}^{-1}$  is tuned to adjust the estimated 0.5 s average lifetime of Ras nanoclusters [15]. Activation frequency at maximal stimulus,  $k_0^{(m)}$ , is arbitrarily fixed to  $1000$   $\text{s}^{-1}$ , so that the average number of simulated nanoclusters is of the order of a few hundreds. This number is well below the typical maximum number of Ras nanocluster in a cell ( $\approx 50$  000) [15] but assures a sufficient statistical ensemble for our stochastic simulations in a reasonable computational time.

### 3. Results

The stimulus/response behaviour of the model is evaluated by representing the velocity  $V_p$  of  $P$  formation normalized

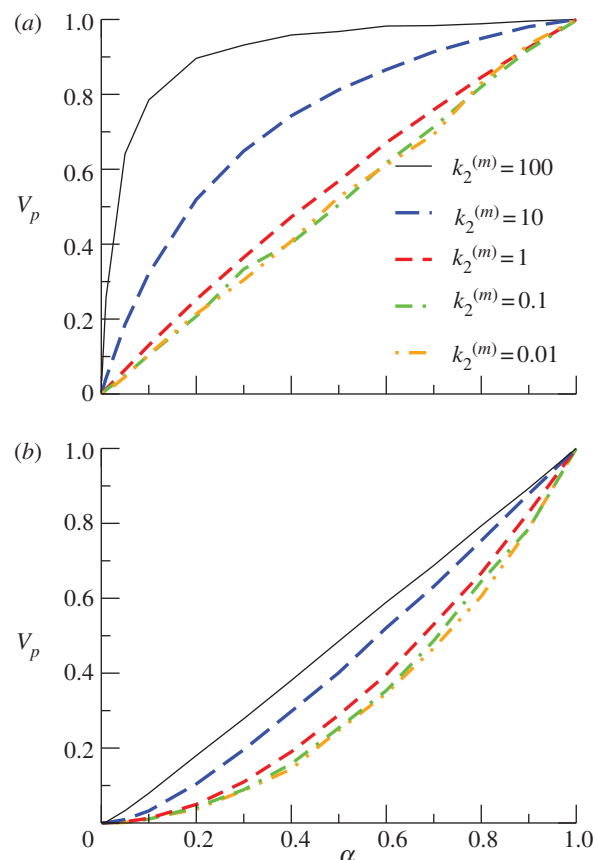


**Figure 3.** Global response  $V_p$  as a function of stimulus  $\alpha$  in model A (external lifetime regulation), for  $k_1 = 1$   $\text{s}^{-1}$ . (a) Number of nanoclusters fixed and independent of the input stimulus ( $k_0 = k_0^{(m)}$ ). (b) Number of nanoclusters regulated by stimulus ( $k_0 = \alpha k_0^{(m)}$ ). (Online version in colour.)

with respect to the maximal production (for  $\alpha = 1$ ) as a function of input stimulus  $\alpha$ . For model A, individual signalling nanoclusters can generate both graded and switch-like outputs (figure 3), depending on the relative values of the reaction rates and whenever nanoclusters do not die too fast,  $k_1 \leq k_3$ . If the limiting reaction is the formation of product molecules from the intermediate complex NC – S,  $k_1 > k_2$ , then nanoclusters generate a graded signal because the impact of the distributive mechanism in the formation of product  $P$  through  $k_2 = \alpha k_2^{(m)}$  becomes relevant. By contrast, for  $k_1 < k_2$ , the limiting reaction is the formation of NC – S. In this situation, once the intermediate complex is formed, product molecules are generated very fast, quite independent of the contribution of the stimulus in the catalytic step. Then, a nanocluster responds maximally to very low inputs (ultrasensitivity) and its output is switch-like, presenting a steeper response for greater differences between  $k_1$  and  $k_2$ . These behaviours are summarized in figure 3a, which reports results from simulations run with a fixed number of operating nanoclusters independent of the input stimulus; namely, for a nanocluster generation rate  $k_0$  fixed to  $k_0^{(m)}$  in order to average a large ensemble of signalling platforms. The stimulus/response curves are plotted for different values of  $k_2^{(m)}$ , given  $k_1 = 1$   $\text{s}^{-1}$ . The global response of the system corresponds to the integration of local signalling events taking place in different activated nanoclusters. In the cell membrane, the number of nanoclusters is proportional to stimulus concentration,  $k_0 = \alpha k_0^{(m)}$  [15]. Figure 3b shows that this global response is nonlinear when the nanoclusters



function in the graded regime (low values of  $k_2^{(m)}$ ), while the system generates a graded, nearly linear product output in the regime of nanoclusters working as nanoswitches (large values of  $k_2^{(m)}$ ), meaning that in this case the signalling response is directly proportional to input stimulus. The fact that nanoclusters respond maximally even at low-stimulus results in a global response only dependent on the number of nanoclusters, proportional to stimulus. This implies that the system of ultrasensitive nanoswitches achieves high-fidelity signal transduction by performing an analogue–digital–analogue transmission [15], an obvious advantage that could be one of the reasons for the active compartmentation of cell signalling processes. We note that our results are obtained for the simplest internal structure of the signalling pathway given in equation (2.1), without the recursion to intricate reactions profuse in biological details.

As an alternative to model A, we propose a signalling mechanism where the nanocluster lifetime is self-regulated via the coupling of nanocluster disassembly to its local activity, without the intervention of external factors (model B, figure 2*b*). We assume that product molecules remain transiently accumulated in a local pool that acts as an internal clock exerting a negative impact on the lifetime of the nanocluster. The more it produced, the higher its chances to die, as happens for instance in Ras–MAPK signalling: production of ERK promotes the phosphorylation of the SOS factor, which inhibits the activity of Ras aggregates [4,7,19]. The concept of local pool is acceptable for short nanocluster lifetimes of fractions of a second. Then, the restricted diffusive motion of product species does not allow them to travel far from the signalling membrane complex. We model the death rate of a nanocluster as  $k_3 P_{nc,i}(t)$ , where  $k_3$  is a constant rate and  $P_{nc,i}(t)$  is the number of signalling product molecules in the local pool generated by the nanocluster  $i$  up to time  $t$ . The latter expression is the simplest dependence for a negative upstream inhibition owing to the final product protein and corresponds to the opposite limit to model A. Whereas model A considers that the dynamics of signalling platforms is completely regulated externally, in model B, this regulation is absolutely modulated by their local activity.

To investigate the impact of local activity regulating the death of nanoclusters, we study the response of model B for the same parameter values used in the simulations of model A in figure 3*a,b*. Lifetime self-regulation enhances nanocluster sensitivity, maintaining the switch-like response for a wider range of values of  $k_2^{(m)}$ , see figure 4*a* for a fixed number of signalling platforms independent of stimulus ( $k_0 = k_0^{(m)}$ ). The explanation is related to the fact that in model B nanoclusters can be active for longer periods when the input signal is low. In model A, most nanoclusters are disassembled before producing any  $P$  molecule when working under a low stimulus. In these cases, and in particular when  $k_2^m$  is small, the effect of the input stimulus in the production of  $P$  becomes critical. Instead, in model B, the death probability of a nanocluster is zero until it has produced at least one  $P$  molecule, so that the second step in equation (2.1) is no longer critical even at low values of  $k_2^{(m)}$ . The latter feature is responsible for enhancing nanocluster ultrasensitivity respect to model A regardless the kinetic conditions of the pathway and/or the input stimulus. In other words, the lifetime of nanoclusters in model B ‘adapts’ to the signalling kinetics to assure the production of one

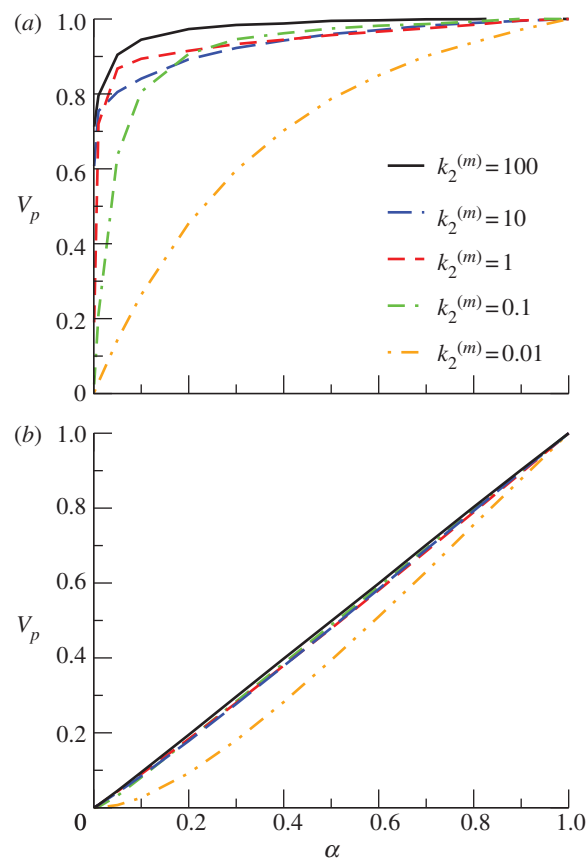


**Figure 4.** Global response  $V_p$  as a function of stimulus  $\alpha$  in model B (lifetime self-regulation), for  $k_1 = 1 \text{ s}^{-1}$ . (a) Number of nanoclusters fixed and independent of the input stimulus ( $k_0 = k_0^{(m)}$ ). (b) Number of nanocluster regulated by stimulus ( $k_0 = \alpha k_0^{(m)}$ ). (Online version in colour.)

product molecule even at low-stimulus and/or slow kinetics, forcing the nanocluster to act as a switch and generate a digital pulse. Note that the lifetimes of nanoclusters are longer in model B at low-input stimulus, they approach the lifetime fixed in model A ( $k_3^{-1}$ ) at moderate stimulus and may become even shorter at maximal stimulus. As a consequence of the gain in nanocluster sensitivity, the global response fidelity is also enhanced in model B, as it is shown in figure 4*b* for simulations using  $k_0 = \alpha k_0^{(m)}$ .

We have also performed a systematic study of signal transmission fidelity in both models at different values of the kinetic rates  $k_1$  and  $k_2^{(m)}$ . Fidelity of signal transduction is quantified here by parameter  $\phi$ , computed as the integral of the global response rescaled by the number of nanoclusters,  $(V_p/\alpha)(\alpha)$ , for the whole range of input stimulus. High-fidelity transduction is achieved when the system response,  $V_p$ , correlates to stimulus,  $\alpha$ , so when  $\phi \rightarrow 1$ . This requires nanoclusters to work in the range where they behave as ultrasensitive nanoswitches. Figure 5 presents the values of  $\phi$  in the  $(k_1, k_2^{(m)})$  parameter space spanning two orders of magnitude for each kinetic rate. Note that high-fidelity signal transmission is a robust feature for the signalling mechanism involving a self-regulated nanocluster dynamics (model B), whereas for the scheme based on a fixed nanocluster lifetime (model A) such virtue requires a fine tuning of the reaction kinetic parameters. A statistical analysis of model robustness in the parameter phase space is not needed because our simple signalling motif only depends on two kinetic parameters ( $k_1$  and  $k_2^{(m)}$ ), so that

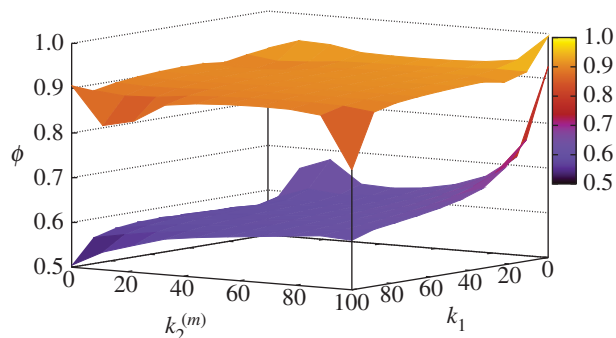


**Figure 5.** Signal transmission fidelity  $\phi$  computed at different values of  $k_1$  and  $k_2^{(m)}$  for models A (bottom surface) and B (top surface). Simulations using  $k_0 = \alpha k_0^{(m)}$ . (Online version in colour.)

the complete information about model robustness is found in figure 5. A possibility to quantify robustness is to compute the ratio  $\Gamma_{\phi'}$  between the parameter space areas where  $\phi > \phi'$  within the total explored parameter area. Considering different  $\phi'$  values, it is shown that model B is much more robust ( $\Gamma_{0.75} = 0.891$ ,  $\Gamma_{0.8} = 0.472$ ,  $\Gamma_{0.85} = 0.158$ ) than model A ( $\Gamma_{0.75} = 0.087$ ,  $\Gamma_{0.8} = 0.046$ ,  $\Gamma_{0.85} = 0.019$ ), presenting 10-fold more surface of the  $\phi$  parameter above the considered threshold values.

## 4. Conclusions

Two important conclusions can be derived from our simulations. First, the sensitivity of signalling platforms is found to be modulated by their lifetime, so it is not exclusively determined by the particular architecture of the signalling pathway as suggested so far. In this respect, the influence of the stimulus in the catalytic step of our approach—potentially reflecting either a distributive phosphorylation mechanism of intermediate kinases or a positive feedback on the activation of Ras signalling—induces an ultrasensitivity response that is, in turn, modulated by the relative values of the kinetic constants. Second, comparison of two extreme models for nanocluster disassembly reveals the importance

of the physical origin of nanocluster lifetime regulation respect to the robustness (i.e. parameter insensitivity) of the signalling mechanisms. As two extreme possibilities, we propose model A where nanocluster lifetime is externally regulated by a fixed frequency, and model B where individual nanocluster activity fully determines its duration. Most likely, biological cell signalling may be regulated by a mixture of these two extreme situations. Importantly, we have shown that any contribution to nanocluster lifetime regulated by local production enhances individual ultrasensitivity outputs, rather independent of the values of the model kinetic parameters. Local negative feedback is shown to assure that signalling nanoclusters work as robust switches, and this underpins high-fidelity global responses that are, consequently, more robust against changes of the kinetic parameters. It could be conjectured, therefore, that nanocluster lifetime self-regulation protects the signalling response from variability in the rates of involved reactions, in the concentration of substrate compounds or in the particular architecture of the signalling pathway.

Many modelling approaches have been attempted to describe cell signalling processes but the complexity of the signalling structure and the number of kinetic parameters hide the particular role of nanocluster dynamics. In this paper, we have proposed a simple and generic signalling motif model that captures essential features of signal transduction, such as ultrasensitiveness and fidelity, and could apply to different types of spatial signalling domains following a temporal birth/death dynamics. Nevertheless, the observed complexity of signalling pathways may entail some biological advantages, for example enabling plasticity to modulate different response amplitudes triggering opposing cell fate decisions within a single cell. In the context of our framework for nanocluster cell signalling, we plan to tackle these questions and others, for example the processing of time-dependent stimulus, in future research.

**Funding statement.** This work was supported by Generalitat de Catalunya grant no. Ref. 2009SGR1055; the Ramón y Cajal program of MICINN; MICINN Project no. BFU2010-21847-C02-02.

## References

- Bhalla US, Iyengar R. 1999 Emergent properties of networks of biological signaling pathways. *Science* **283**, 381–387. (doi:10.1126/science.283.5400.381)
- Brightman FA, Fell DA. 2000 Differential feedback regulation of the MAPK cascade underlies the quantitative differences in EGF and NGF signaling in PC12 cells. *FEBS Lett.* **482**, 169–174. (doi:10.1016/S0014-5793(00)02037-8)
- Schoeberl B, Eichler-Jonsson C, Gilles ED, Müller G. 2002 Computational modeling of the dynamics of the MAP kinase cascade activated by surface and internalized EGF receptors. *Nat. Biotechnol.* **20**, 370–375. (doi:10.1038/nbt0402-370)
- Shin S-Y, Rath O, Choo S-M, Fee F, McFerran B, Kolch W, Cho K-H. 2009 Positive- and negative-feedback regulations coordinate the dynamic behavior of the Ras–Raf–MEK–ERK signal transduction pathway. *J. Cell Sci.* **122**, 425–435. (doi:10.1242/jcs.036319)
- de Ronde W, Tostevin F, ten Wolde PR. 2011 Multiplexing biochemical signals. *Phys. Rev. Lett.* **107**, 04810. (doi:10.1103/PhysRevLett.107.048101)
- Andreu-Pérez P *et al.* 2011 Protein arginine methyltransferase 5 regulates ERK1/2 signal transduction amplitude and cell fate through CRAF. *Sci. Signal.* **4**, 190 ra58. (doi:10.1126/scisignal.2001936)
- Kolch W. 2000 Meaningful relationships: the regulation of the Ras/Raf/MEK/ERK pathway by protein interactions. *Biochem. J.* **351**, 289–305. (doi:10.1042/0264-6021:3510289)
- Dhillon AS, Hagan S, Rath O, Kolch W. 2007 MAP kinase signaling pathways in cancer. *Oncogene* **26**, 3279–3290. (doi:10.1038/sj.onc.1210421)
- Huang CY, Ferrell JE. 1996 Ultrasensitivity in the mitogen-activated protein kinase cascade. *Proc. Natl Acad. Sci. USA* **93**, 10 078–10 083. (doi:10.1073/pnas.93.19.10078)
- Kholodenko BN. 2000 Negative feedback and ultrasensitivity can bring about oscillations in the mitogen-activated protein kinase cascades. *Eur. J. Biochem.* **267**, 1583–1588. (doi:10.1046/j.1432-1327.2000.01197.x)
- Sturm OE *et al.* 2010 The mammalian MAPK/ERK pathway exhibits properties of a negative feedback amplifier. *Sci. Signal.* **3**, ra90. (doi:10.1126/scisignal.2001212)
- Henis YI, Hancock JF, Prior IA. 2009 Ras acylation, compartmentalization and signalling nanoclusters. *Mol. Membr. Biol.* **26**, 80–92. (doi:10.1080/09687680802649582)

13. Kholodenko BN, Hancock JF, Kolch W. 2010 Signalling ballet in space and time. *Nat. Rev. Mol. Cell Biol.* **11**, 414–426. (doi:10.1038/nrm2901)
14. Harding AS, Hancock JF. 2008 Using plasma membrane nanoclusters to build better signaling circuits. *Trends Cell Biol.* **18**, 364–371. (doi:10.1016/j.tcb.2008.05.006)
15. Tian T, Harding A, Inder K, Plowman S, Parton RG, Hancock JF. 2007 Plasma membrane nanoswitches generate high-fidelity Ras signal transduction. *Nat. Cell Biol.* **9**, 905–914. (doi:10.1038/ncb1615)
16. Boykevich S, Zhao C, Sondermann H, Philippidou P, Haleboua S, Kuriyan J, Bar-Sagi D. 2006 Regulation of Ras signaling dynamics by SOS-mediated positive feedback. *Curr. Biol.* **16**, 2173–2179. (doi:10.1016/j.cub.2006.09.033)
17. Gillespie DT. 1976 A general method for numerically simulating the stochastic evolution of coupled chemical reactions. *J. Comput. Phys.* **22**, 403–434. (doi:10.1016/0021-9991(76)90041-3)
18. Gillespie DT. 1977 Exact stochastic simulation of coupled chemical reactions. *J. Phys. Chem.* **81**, 2340–2361. (doi:10.1021/j100540a008)
19. Kamioka Y, Yasuda S, Fujita Y, Aoki K, Matsuda M. 2010 Multiple decisive phosphorylation sites for the negative feedback regulation of SOS1 via ERK\*. *J. Biol. Chem.* **285**, 33 540–33 548. (doi:10.1074/jbc.M110.135517)